Chapter 3

Planar Zoom Module

Various applications of planar optics have been presented in the fields of optical computing, communication, information processing, storage system and so on. Herein, another example of planar zoom module is proposed for the application of laser beam scaling. Its design and applications will be described in this chapter.

Conventionally, a zoom lens performs the zoom function by adjusting its position along the optical axis (longitudinal direction); thus, it requires sufficient volume for the motion of the lens. In 2001, a transverse zoom lens set was designed to reduce the volume through the motion or rotation of the lens set along the direction normal to the optical axis.[1] However, because the transverse zoom lens requires several sets of discrete lenses, it is still not sufficiently compact. According to the planar optics,[2] we proposed a novel planar zoom module (PZM) for efficiently reducing the volume of the optical zoom lens set. Moreover, on the basis of PZM, we designed a beam expander with the advantages of multi-magnification and compact volume.

In this chapter, we will describe the model of a PZM, followed by discussions of the theory, analyses, and the considerations in the fabrication of a multi-magnification beam expander application.

3.1 Model of Planar Zoom Module (PZM)

Recall the characteristics of planar optics, which are the folded optical path and the free-space optical elements located on surfaces of the substrate.[2] According to these concepts, the major optical elements of a PZM, such as lenses and mirrors, are designed on properly profiled and coated surfaces of the substrate. An illustration is shown in Fig. 3-1, where the optical elements on a PZM are indicated as D_1, D_2, D_3. . .

etc. We design the input element D_1 and the output element D_4 as transparent elements for the transmission of light, while the other intermediate ones are reflective elements to realize the folded optical path. As a result, the PZM can perform the functions of zoom and compensation by elaborately assembling optical elements together.

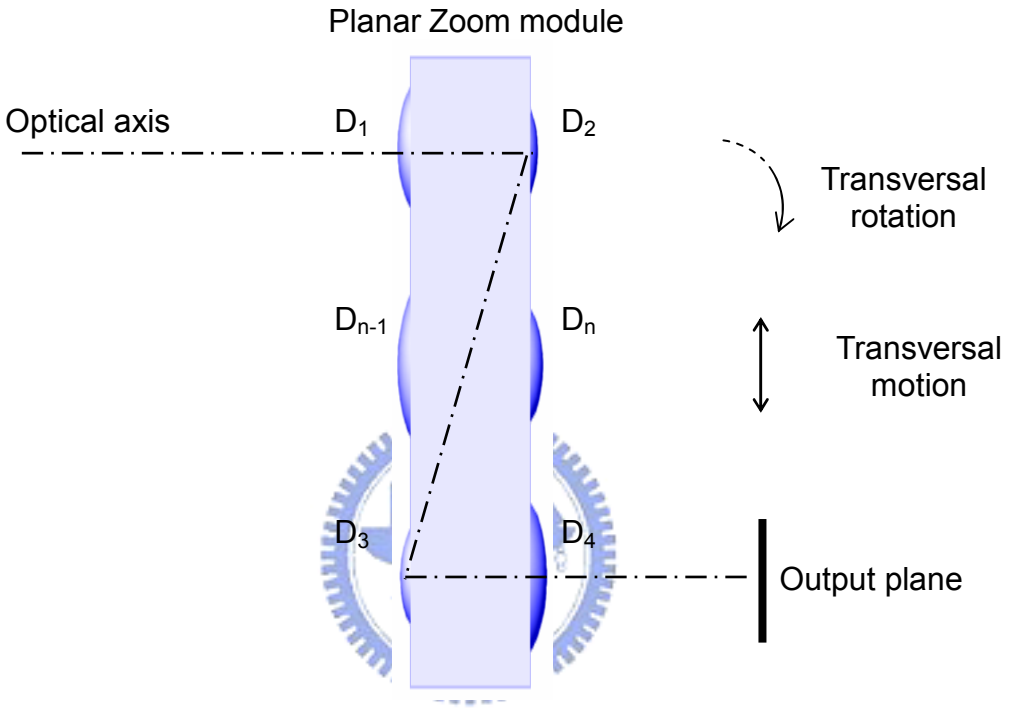

Fig. 3-1 Side view of a planar zoom lens system.

Consider a proper substrate adaptable to the light source. When the incident light passes through D_1, it will be reflected by D_2 and other reflective elements along the optical path in turn. Then it will pass through D_4 and reaches the output plane. Assign the above sequence as the first configuration of the PZM, the effective focal length as f_{e1}, and the corresponding magnification as M_1. Thereby, M_1 is the synergetic result of all elements along the optical path of the first configuration, as shown in Fig. 3-2(a). By the transverse motion or rotation of a PZM, the configuration will be changed to the second, third. . . or other configurations, which are designed with different effective focal lengths f_{e2}, f_{e3}. . . and magnifications M_2, M_3. . ., as illustrated in Fig.

3-2(b). Therefore, the PZM performs the function of zoom lens with discrete zooming.

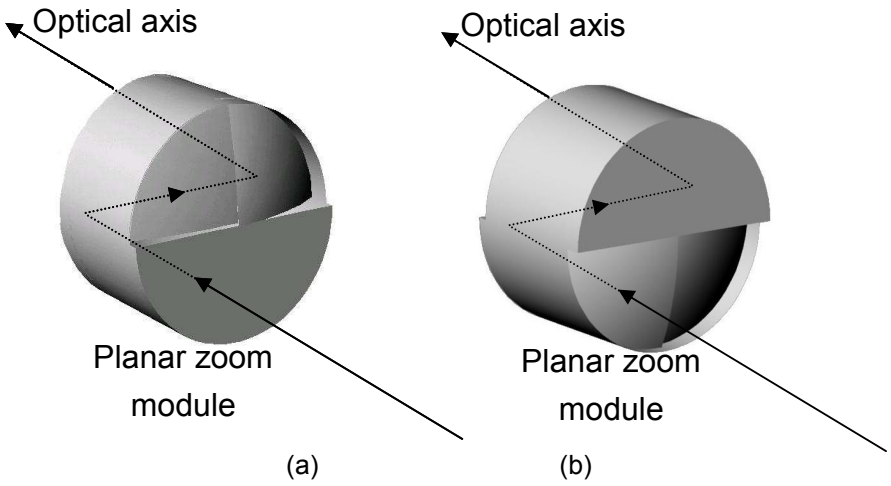

Fig. 3-2 Perspective view of a planar zoom lens system: (a) the 1st and (b) the 2nd configurations.

3.2 Theory of Beam Expander

In this section, we will elucidate the application of PZM to a beam expander. Consider a collimated beam which is incident to a pair of mirrors, D_a and D_b, as shown in Fig. 3-3. Assume that D_a and D_b are separated with a distance of d along the common optical axis, and their focal lengths are f_a and f_b, respectively.

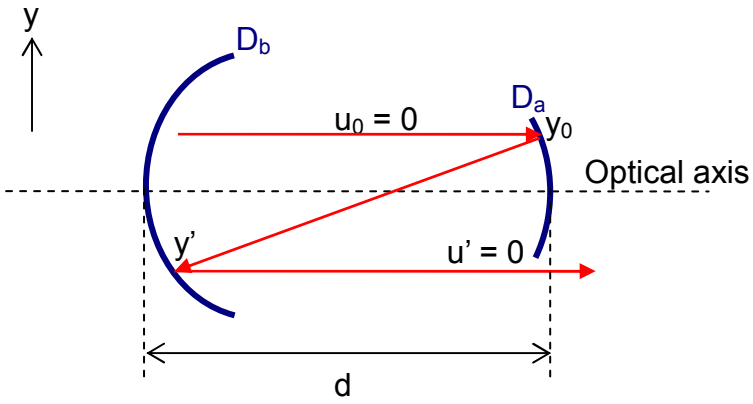

Fig. 3-3 Two-mirror structure of a beam expander.

According to the ABCD matrix theory, the transfer matrix resulting from D_a and D_b is given by

$$T = \begin{bmatrix} 1 & \frac{-1}{|f_b|} \\ 0 & 1 \end{bmatrix} \cdot \begin{bmatrix} 1 & 0 \\ d & 1 \end{bmatrix} \cdot \begin{bmatrix} 1 & \frac{-1}{|f_a|} \\ 0 & 1 \end{bmatrix}, \tag{3-1}$$

If an incident ray is with a height of $y_0 = y$ and the incident slope of $u_0 = 0$, the outcome should be:

$$\begin{bmatrix} u' \\ y' \end{bmatrix} = T \cdot \begin{bmatrix} 0 \\ y \end{bmatrix}, \tag{3-2}$$

where *y'* is the height of the exit ray and *u'* is the exit slope which is assumed to be 0. With the magnification *m* defined as the ratio of the height of the outcome to that of the incident ray, we obtain:

$$u' = 0, \tag{3-3}$$

$$y' = my. \tag{3-4}$$

By substituting eqs. (3-3) and (3-4) into eqs. (3-1) and (3-2), design formulas can be derived:

$$|f_a| + |f_b| = d, \tag{3-5}$$

$$m = -|f_b| / |f_a|. \tag{3-6}$$

Equations (3-5) and (3-6) show that the on-axis zooming, i.e. $u' = u_0 = 0$, can be realized by two confocal mirrors while magnification equalizes to the ratio of their focal lengths. By mapping this structure to a PZM, we design a beam expander illustrated in Fig. 3-4, where there are two configurations with eight elements.

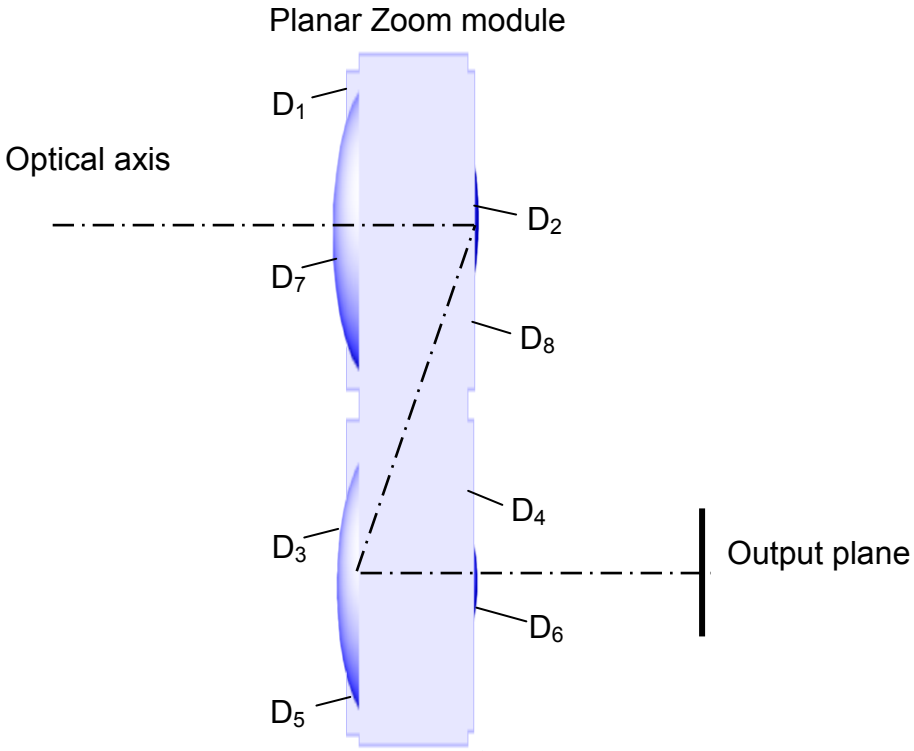

Fig. 3-4 Side view of a multi-magnification beam expander.

Magnification can be altered by the transverse rotation of the PZM, as shown in Fig. 3-5. Both the front and the rear surfaces of the substrate are divided into four parts to obtain eight elements, labeled as D_1, D_2,. . . D_8. The first configuration for zooming consists of D_1, D_2, D_3, and D_4, while the second configuration consists of D_5, D_6, D_7, and D_8. Meanwhile, D_1, D_4, D_5, and D_8 are designed as transparent elements. Input elements, D_1 and D_5, can have flat surfaces for transmitting the collimated beams or Fresnel lenses for collimating incident lights. Output elements, D_4 and D_8, can also have flat surfaces for transmitting the exit collimated beams or Fresnel lenses for focusing the outcome to the destination.

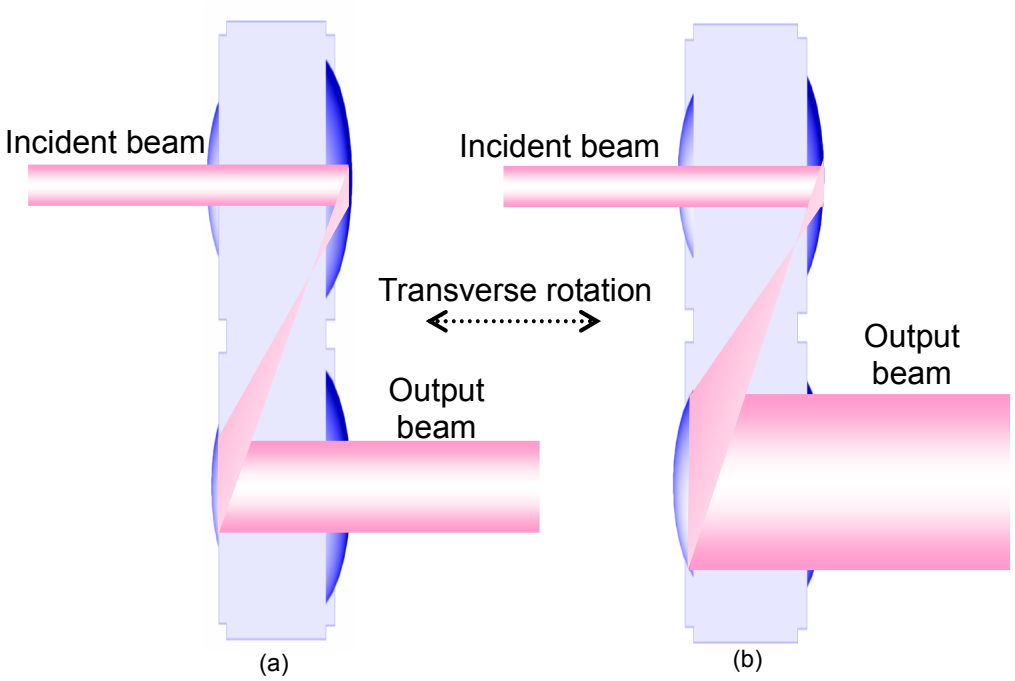

Fig. 3-5 Side view of varying the magnification between (a) the 1st and (b) the 2nd configurations.

To design D_2, D_3, D_6, and D_7, we apply eqs. (3-5) and (3-6). Then, the magnifications of the first and second configurations, M_1 and M_2, respectively, are:

$$M_1 = -|f_3|/|f_2|, \tag{3-7}$$

$$M_2 = -|f_7|/|f_6|, \tag{3-8}$$

with

$$|f_2| + |f_3| = d, \tag{3-9}$$

$$|f_6| + |f_7| = d. \tag{3-10}$$

Moreover, since the paraboloid mirror for collimated beams has the inherent merits of being chromatic aberration free[3] and spherical aberration free,[4] D_2, D_3, D_6, and D_7 are designed as not only confocal but also paraboloid mirrors so that a multi-magnification beam expander modulated by rotation can be realized without chromatic or spherical aberrations.

3.3 Analysis of Beam Expander

3.3.1 Discussion on aberrations

Seidel aberrations, also called primary aberrations, affect the functions of the beam expander. Because of the folded optical path, primary oblique aberrations such as coma, astigmatism and distortion must be carefully considered in a PZM. With appropriate compensation methods,[5] these aberrations can be eliminated or neglected. Our design is also an example. That is, because the slopes of the incident and the exit beams are zero, i.e. $u' = u_0 = 0$, there will be no oblique aberrations. Along with the merits of paraboloid mirrors (preventing collimated beams from chromatic and spherical aberrations), this multi-magnification beam expander based on a PZM is, therefore, theoretically free from primary aberrations. It is noted that the designed beam expander can be applied to not only monochromatic beams but also white lights with extremely small aberrations.

3.3.2 Simulation results

According to above discussions, we demonstrated the PZM as a multi-magnification beam expander by simulation.

Assume the glass substrate with the refractive index $n = 1.5$, thickness $d = 15$ mm, two configurations with the magnifications of $M_1 = -2$ and $M_2 = -4$. For simplicity, D_1, D_4, D_5, and D_8 are assigned as flat transparent elements. By the substitution of M_1, M_2 and d in eqs. (3-7)–(3-10), the focal lengths of the paraboloid mirrors can be calculated as $f_2 = -5$ mm, $f_3 = 10$ mm, $f_6 = -3$ mm, and $f_7 = 12$ mm.

By arranging aperture stops with the radii of 2 mm at the centers of D_1 and D_5, and aperture sizes with the radii of 10 mm for the other six elements, we simulated the system by OSLO. The ray tracing results are shown in Figs.3-6 (a) and (b) for the first and second configurations, respectively. As shown in Figs.3-6 (a) and (b), the diameters of output beams are twice and four times as large as that of the input,

respectively. Consequently, the function of multi-magnification is realized. In addition, the paraxial analysis under the visible spectrum shows that the worst Seidel aberration coefficient is Petzval field curvature with the angular displacement (direction tangent) of less than 10^{-12}. Thus, the numerical values of aberrations are shown to be negligible.

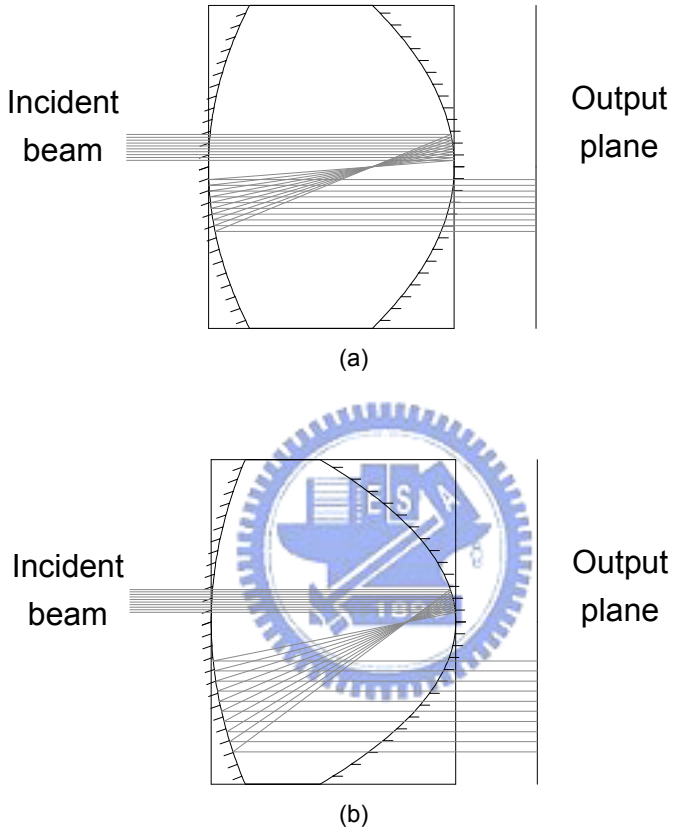

Fig. 3-6 Ray tracing results of the (a) 1st and (b) 2nd configurations.

3.4 Fabrication Considerations

3.4.1 Dimensions of elements

In our design of the beam expander, element size can be reduced by adequately matching with beam size. This approach can efficiently save fabrication time and reduce cost. Next, we will define the dimension of each element on the beam expander.

Figure 3-7 shows the structure of the first configuration of the beam expander. D_1 and D_4 are flat and transparent elements, while the paraboloid mirrors D_2 and D_3 are

spherical paraboloids with both focal points at the origin. Then, only the y-axis and z-axis shall be taken into account.

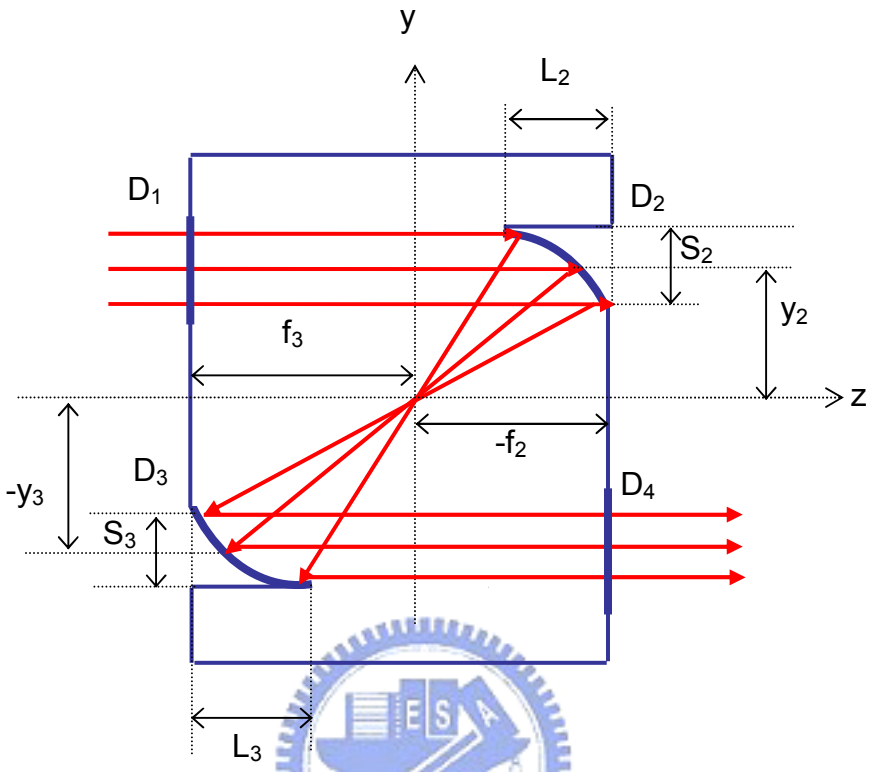

Fig. 3-7 Dimensions of the element for the 1st configuration.

The shape function of D_2 can be written as:

$$y^2 = 4f_2(z + f_2), \tag{11}$$

where f_2 is the focal length of D_2 and has a negative value. The shape function of D_3 is:

$$y^2 = 4f_3(z + f_3), \tag{12}$$

where f_3 is the focal length of D_3 and has a positive value. If the aperture stop lies in the primary mirror D_2 with the diameter S_2, and the central height of D_2 is y_2, then the depth of D_2 along the z direction, L_2, can be derived by the shape function:

$$L_2 = \frac{y_2 S_2}{2|f_2|}. \tag{13}$$

Because of the magnification M_1, the diameter of D_3, labeled as S_3, should be

$$S_3 \geq |M_1| S_2 . \tag{14}$$

Moreover, the central height and the depth of D_3, labeled as $-y_3$ and L_3 in Fig. 3-7, respectively, can be derived from the geometry and eqs. (3-7), (3-12) and (3-14):

$$y_3 = -|M_1| y_2 , \tag{15}$$

$$L_3 = \frac{-y_3 S_3}{2f_3} \geq \frac{M_1^2 y_2 S_2}{2f_3} = |M_1| L_2 . \tag{16}$$

Equations (3-13) and (3-16) show that the dimension of an element is dependent on its focal length, the magnification, and the diameter and central position of the primary paraboloid mirror. Likewise, one can decide the sizes of elements for other configurations. It can be concluded that the beam expander can be fabricated in both macro- and micro-schemes by appropriately scaling the diameter and central position of the primary paraboloid mirror.

3.4.2 Sorts of beam expander

According to the fabrication strategies, we may classify the beam expander into three types: the continuous-surface, the diffractive optical element (DOE), and the hybrid devices. The above discussions and simulations are based on the continuous-surface device, so that the paraboloid mirrors bring many advantages, particularly wavelength independence and high efficiency. Since the aspherical surfaces, paraboloid mirrors, are needed in our applications, we may use fabrication processes such as precision diamond turning or grinding to yield high-quality optical surfaces. However, a subsequent polishing process is required to remove the tool marks of these techniques. Thus, controlling the polishing process for better surface roughness becomes an important issue.[6] When massive fabrication is considered,

glass molding is normally used, but it has a lower size limit of 1mm for the diameter of the lens.[7] In other words, for the macro-optics at a diameter larger than 1 mm, current fabrication techniques are sufficiently developed.

A glass molding technique, named mold process lens (MPL), has been proposed for the fabrication of a miniatured aspherical lens with an effective diameter of 0.211mm.[7] Another technique called gray-scale mask lithography has been also a candidate for making the continuous-surface beam expander, due to its high potential of being compatible with the VLSI technology (standard semiconductor process) and one-time exposure.[8] Nevertheless, it may not yield the thick and smooth aspherical optics when the continuous-surface device has a too large depth. Currently, advanced techniques, such as the ultra-precision machining with single-point diamond tools, are available to fabricate surfaces with the form error of less than 0.1μm and the roughness of less than 0.010μm.[9] Thus, it is promising to shrink the dimensions of continuous-surface PZM to the micro scale for those high-resolution applications, such as the example shown in section 6.2.1. When a PZM is shrunk to the scale near the wavelength, it shall be noted that the demonstrated ray tracing model might not have sufficient accuracy; then the modeling shall refer to other less-approximation algorithms, such as diffraction theories.

Due to the planar structure of the planar zoom module, one can transform the designed surface profile to the profile of a DOE, such as a Fresnel lens. Such DOE devices can be fabricated by the planar integration technology, e.g. the standard VLSI technology. Since the conventional DOE is quantized with multiple phase levels related to the specific wavelength, its non-continuous surface profile will decrease output efficiency and the DOE will be wavelength-dependent. However, when applied to a laser beam expander, such a DOE device could be an appropriate solution.

Another type of the hybrid device is the combination of the continuous-surface

and the DOE types. As shown in Fig. 3-8, a continuous-surface paraboloid profile can be transformed to a quasi-DOE with a period of several times that of the designed wavelength, so that only the inner part of each order (zone) keeps the shape of paraboloid and the thickness of the paraboloid mirror is reduced. Although this scheme is still wavelength-dependent, it gains higher output efficiency when compared with the conventional DOE device; it is also suitable for VLSI-compatible processes such as gray-scale mask lithography.

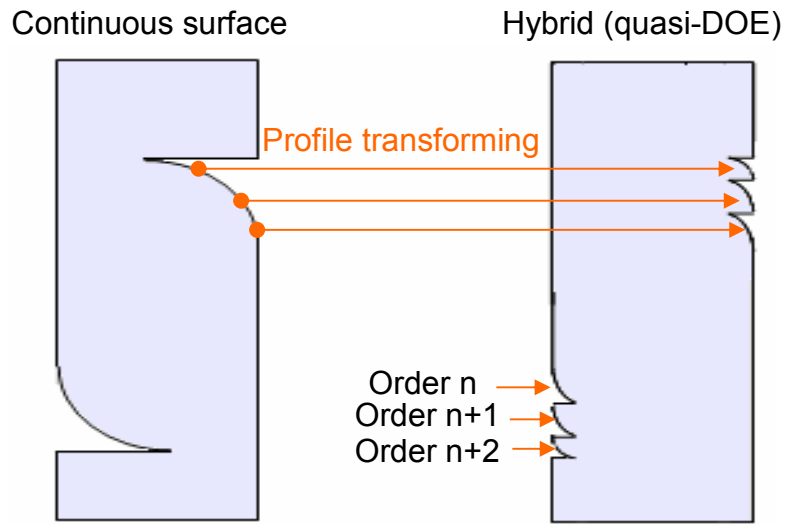

Fig. 3-8 Transformation from a continuous-surface device to a hybrid device. The continuous profile is transformed to multiple zones of profiles.

Using the above-mentioned methods, the designed beam expander and even other PZMs can be fabricated from macro- to micro- optics with the advantages of light weight and small size.

3.5 Summary

We have presented a model of a planar zoom module (PZM), used it as a multi-magnification beam expander, and derived the design formulas for the beam expander. The analyses and simulation results show that the aberrations of such beam

expander are negligible. Meanwhile, according to the analyses of dimensions of elements and fabrication schemes, the PZM shall be able to be realized from macro to micro dimensions with the advantage of compactness.

3.6 Reference

[1] R.-S. Chang, U.S. Patent 6278558 B1 (2001)

[2] J. Jahns and A. Huang, Appl. Opt. **28** 1602-1605 (1989).

[3] R. E. Fischer and B. Tadic-Galeb, *Optical System Design*, Ch7 and 8, McGraw-Hill, (2001).

[4] D. Malacara and Z. Malacara, *Handbook of lens design*, Ch 5, Marcel Dekker, Inc., (1994).

[5] M. Testorf and J. Jahns, J. Opt. Soc. Am. A **16**, 1175-1183 (1999).

[6] M. Y. Yang and H. C. Lee, J. Mater. Process. Tech. **116**, 298-304 (2001).

[7] M. Yamada, T. Miura, H. Sakakibara, S. Aoki, T. Kanazawa and T. Watanabe, Jpn. J. Appl. Phys. **42**, 895-897 (2003).

[8] S. H. Lee, M. S. Jin and M. L. Scott, U.S. Patent 6534221 B2 (2003).

[9] http://blog.sina.com.tw/tool/